

Sudden reversal in the pressure dependence of T_c in the iron-based superconductor CsFe_2As_2 : A possible link between inelastic scattering and pairing symmetry

F. F. Tafti,^{1,*} J. P. Clancy,² M. Lapointe-Major,¹ C. Collignon,¹ S. Faucher,¹
 J. A. Sears,² A. Juneau-Fecteau,¹ N. Doiron-Leyraud,¹ A. F. Wang,³ X.-G. Luo,³
 X. H. Chen,³ S. Desgreniers,⁴ Young-June Kim,² and Louis Taillefer^{1,5,†}

¹*Département de physique & RQMP, Université de Sherbrooke, Sherbrooke, QC, Canada*

²*Department of Physics, University of Toronto, Toronto, ON, Canada*

³*Hefei National Laboratory for Physical Sciences at Microscale and Department of Physics, University of Science and Technology of China, Hefei, Anhui 230026, China*

⁴*Faculty of Science, University of Ottawa, Ottawa, ON, Canada*

⁵*Canadian Institute for Advanced Research, Toronto, ON, Canada*

(Dated: September 21, 2018)

We report a sudden reversal in the pressure dependence of T_c in the iron-based superconductor CsFe_2As_2 , similar to that discovered recently in KFe_2As_2 [Tafti *et al.*, Nat. Phys. **9**, 349 (2013)]. As in KFe_2As_2 , we observe no change in the Hall coefficient at $T \rightarrow 0$, again ruling out a Lifshitz transition across the critical pressure P_c . We interpret the T_c reversal in the two materials as a phase transition from one pairing state to another, tuned by pressure, and we investigate what parameters control this transition. Comparing samples of different residual resistivity ρ_0 , we find that a 6-fold increase in impurity scattering does not shift P_c . From a study of X-ray diffraction on KFe_2As_2 under pressure, we report the pressure dependence of lattice constants and As-Fe-As bond angle. The pressure dependence of the various lattice parameters suggests that P_c should be significantly higher in CsFe_2As_2 than in KFe_2As_2 , but we find on the contrary that P_c is lower in CsFe_2As_2 , indicating that other factors control T_c . Resistivity measurements under pressure reveal a change of regime across P_c , suggesting a possible link between inelastic scattering and pairing symmetry.

PACS numbers: 74.70.Xa, 74.62.Fj, 61.50.Ks

I. INTRODUCTION

To understand what controls T_c in high temperature superconductors remains a major challenge. Several studies suggest that in contrast to cuprates where chemical substitution controls electron concentration, the dominant effect of chemical substitution in iron-based superconductors is to tune the structural parameters – such as the As-Fe-As bond angle – which in turn control T_c .^{1,2} This idea is supported by the parallel tuning of T_c and the structural parameters of the 122 parent compounds BaFe_2As_2 and SrFe_2As_2 .^{3,4} In the case of $\text{Ba}_{1-x}\text{K}_x\text{Fe}_2\text{As}_2$, at optimal doping ($x = 0.4$, $T_c = 38$ K) the As-Fe-As bond angle is $\alpha = 109.5^\circ$, the ideal angle of a non-distorted FeAs_4 tetrahedral coordination. Underdoping, overdoping, or pressure would tune the bond angle away from this ideal value and reduce T_c by changing the electronic bandwidth and the nesting conditions.³

CsFe_2As_2 is an iron-based superconductor with $T_c = 1.8$ K and $H_{c2} = 1.4$ T.^{5–7} Based on the available X-ray data,⁵ the As-Fe-As bond angle in CsFe_2As_2 is 109.58° , close to the ideal bond angle that yields $T_c = 38$ K in optimally-doped $\text{Ba}_{0.6}\text{K}_{0.4}\text{Fe}_2\text{As}_2$. If the bond angle were the key tuning factor for T_c , CsFe_2As_2 should have a much higher transition temperature than 1.8 K.

In this article, we show evidence that T_c in $(\text{K,Cs})\text{Fe}_2\text{As}_2$ may be controlled by details of the inelastic scattering processes that are not directly related to

structural parameters, but are encoded in the electrical resistivity $\rho(T)$. The importance of inter- and intra-band inelastic scattering processes in determining T_c and the pairing symmetry of iron pnictides has been emphasized in several theoretical works.^{8–10} Recently, it was shown that a change of pairing symmetry can be induced by tuning the relative strength of different competing inelastic scattering processes, *i.e.* different magnetic fluctuation wavevectors.¹¹

In a previous paper, we reported the discovery of a sharp reversal in the pressure dependence of T_c in KFe_2As_2 , the fully hole-doped member of the $\text{Ba}_{1-x}\text{K}_x\text{Fe}_2\text{As}_2$ series.¹² No sudden change was observed in the Hall coefficient or resistivity across the critical pressure $P_c = 17.5$ kbar, indicating that the transition is not triggered by a change in the Fermi surface. Recent dHvA experiments under pressure confirm that the Fermi surface is the same on both sides of P_c , ruling out a Lifshitz transition and strengthening the case for a change of pairing state.¹³ We interpret the sharp T_c reversal as a phase transition from d -wave to s -wave symmetry. Bulk measurements such as thermal conductivity^{14,15} and penetration depth¹⁶ favor d -wave symmetry at zero pressure. Because the high-pressure phase is very sensitive to disorder, a likely s -wave state is one that changes sign around the Fermi surface, as in the s_\pm state that changes sign between the Γ -centered hole pockets, as proposed by Maiti *et al.*¹⁰ It appears that in KFe_2As_2 s -wave and d -wave states are nearly degenerate, and a small pressure is

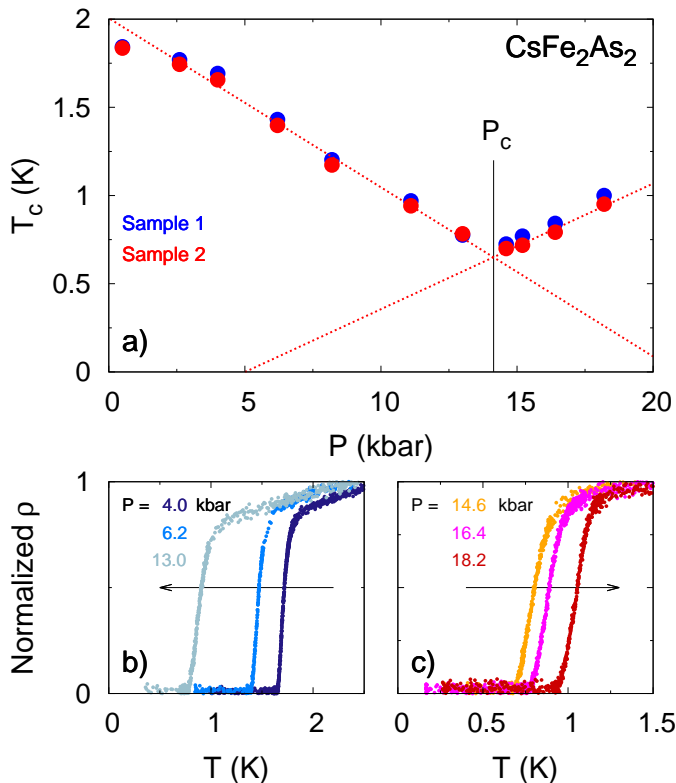


FIG. 1. a) Pressure dependence of T_c in CsFe_2As_2 . The blue and red circles represent data from samples 1 and 2, respectively. T_c is defined as the temperature where the zero-field resistivity $\rho(T)$ goes to zero. The critical pressure P_c marks a change of behaviour from decreasing to increasing T_c . Dotted red lines are linear fits to the data from sample 2 in the range $P_c - 10$ kbar and $P_c + 5$ kbar. The critical pressure $P_c = 14 \pm 1$ kbar is defined as the intersection of the two linear fits. b) Low-temperature $\rho(T)$ data, from sample 2, normalized to unity at $T = 2.5$ K. Three isobars are shown at $P < P_c$, with pressure values as indicated. The arrow shows that T_c decreases with increasing pressure. c) Same as in b), but for $P > P_c$, with ρ normalized to unity at $T = 1.5$ K. The arrow shows that T_c now *increases* with increasing pressure.

enough the push the system from one state to the other.

In this article, we report the discovery of a similar T_c reversal in CsFe_2As_2 . The two systems have the same tetragonal structure, but their lattice parameters are notably different.⁵ Our high-pressure X-ray data reveal that at least 30 kbar of pressure is required for the lattice parameters of CsFe_2As_2 to match those of KFe_2As_2 . Yet, surprisingly, we find that P_c is *smaller* in CsFe_2As_2 than in KFe_2As_2 . This observation clearly shows that structural parameters alone are not the controlling factors for P_c in $(\text{K,Cs})\text{Fe}_2\text{As}_2$. Instead, we propose that competing inelastic scattering processes are responsible for tipping the balance between pairing symmetries.

II. EXPERIMENTS

Single crystals of CsFe_2As_2 were grown using a self-flux method.⁷ Resistivity and Hall measurements were performed in an adiabatic demagnetization refrigerator, on samples placed inside a clamp cell, using a six-contact configuration. Hall voltage is measured at plus and minus 10 T from $T = 20$ to 0.2 K and antisymmetrized to calculate the Hall coefficient R_H . Pressures up to 20 kbar were applied and measured with a precision of ± 0.1 kbar by monitoring the superconducting transition temperature of a lead gauge placed besides the samples inside the clamp cell. A pentane mixture was used as the pressure medium. Two samples of CsFe_2As_2 , labelled “sample 1” and “sample 2”, were measured and excellent reproducibility was observed.

High pressure X-ray experiments were performed on polycrystalline powder specimens of KFe_2As_2 up to 60 kbar with the HXMA beam line at the Canadian Light Source, using a diamond anvil cell with silicon oil as the pressure medium. Pressure was tuned blue with a precision of ± 2 kbar using the R_1 fluorescent line of a ruby chip placed inside the sample space. XRD data were collected using angle-dispersive techniques, employing high energy X-rays ($E_i = 24.35$ keV) and a Mar345 image plate detector. Structural parameters were extracted from full profile Rietveld refinement using the GSAS software.¹⁷ Representative refinements of the X-ray data are presented in appendix A.

III. RESULTS

Fig. 1a shows our discovery of a sudden reversal in the pressure dependence of T_c in CsFe_2As_2 at a critical pressure $P_c = 14 \pm 1$ kbar. The shift of T_c as a function of pressure clearly changes direction from decreasing (Fig. 1b) to increasing (Fig. 1c) across the critical pressure P_c . T_c varies linearly near P_c , resulting in a V-shaped phase diagram similar to that of KFe_2As_2 .¹²

Measurements of the Hall coefficient R_H allow us to rule out the possibility of a Lifshitz transition, *i.e.* a sudden change in the Fermi surface topology. Fig. 2 shows the temperature dependence of R_H at five different pressures. In the zero-temperature limit, $R_H(T \rightarrow 0)$ is seen to remain unchanged across P_c (Fig. 2, inset). If the Fermi surface underwent a change, such as the disappearance of one sheet, this would affect $R_H(T \rightarrow 0)$, which is a weighted average of the Hall response of the various sheets. Similar Hall measurements were also used to rule out a Lifshitz transition in KFe_2As_2 ,¹² in agreement with the lack of any change in dHvA frequencies.¹³

Several studies on the $\text{Ba}_{1-x}\text{K}_x\text{Fe}_2\text{As}_2$ series suggest that lattice parameters, in particular the As-Fe-As bond angle, control T_c .^{2-4,18} To explore this hypothesis, we measured the lattice parameters of KFe_2As_2 as a function of pressure, up to 60 kbar, in order to find out how much pressure is required to tune the lattice param-

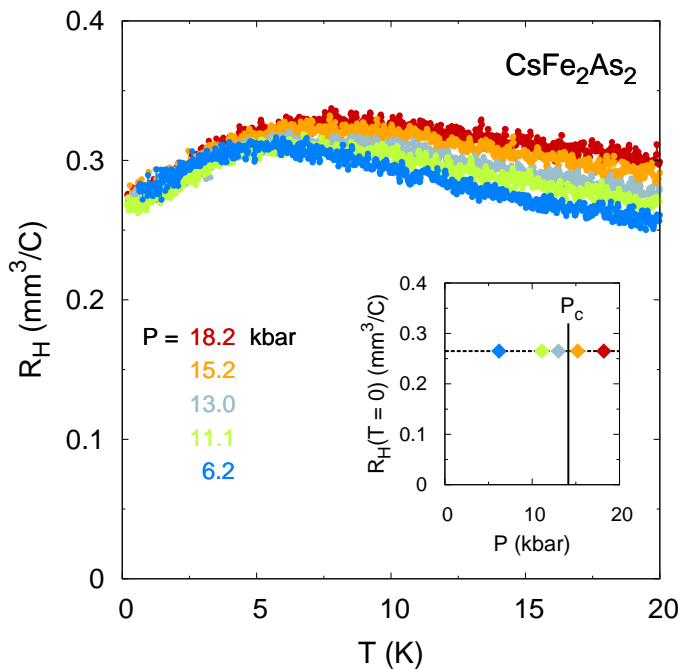


FIG. 2. Temperature dependence of the Hall coefficient $R_H(T)$ in CsFe_2As_2 (sample 2), at five selected pressures, as indicated. The low-temperature data converge to the same value for all pressures, whether below or above P_c . *Inset*: The value of R_H extrapolated to $T = 0$ is plotted at different pressures. Horizontal and vertical error bars are smaller than symbol dimensions. $R_H(T = 0)$ is seen to remain unchanged across P_c .

ters of CsFe_2As_2 so they match those of KFe_2As_2 . Cs has a larger atomic size than K, hence one can view CsFe_2As_2 as a negative-pressure version of KFe_2As_2 . The four panels of Fig. 3 show the pressure variation of the lattice constants a and c , the unit cell volume ($V = a^2c$), and the intra-planar As-Fe-As bond angle (α) in KFe_2As_2 . The red horizontal line in each panel marks the value of the corresponding lattice parameter in CsFe_2As_2 .⁵ In order to tune a , c , V , and α in KFe_2As_2 to match the corresponding values in CsFe_2As_2 , a negative pressure of approximately -10 , -75 , -30 , and -30 kbar is required, respectively. Adding these numbers to the critical pressure for KFe_2As_2 ($P_c = 17.5$ kbar), we would naively estimate that the critical pressure in CsFe_2As_2 should be $P_c \simeq 30$ kbar or higher. We find instead that $P_c = 14$ kbar, showing that other factors are involved in controlling P_c .

It is possible that the lower P_c in CsFe_2As_2 could be due to the fact that T_c itself is lower than in KFe_2As_2 at zero pressure, *i.e.* that the low-pressure phase is weaker in CsFe_2As_2 . One hypothesis for the lower T_c in CsFe_2As_2 is a higher level of disorder. To test this idea, we studied the pressure dependence of T_c in a less pure KFe_2As_2 sample. Fig. 4 compares the T - P phase diagram in three samples: 1) a high-purity KFe_2As_2 sample, with $\rho_0 = 0.2 \mu\Omega \text{ cm}$ (from ref. 12); 2) a less pure KFe_2As_2 sample, with $\rho_0 =$

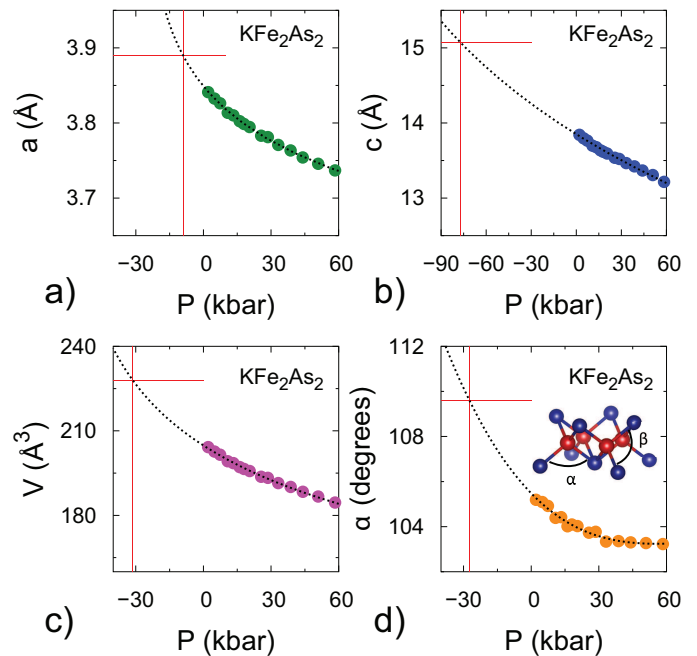


FIG. 3. Structural parameters of KFe_2As_2 as a function of pressure, up to 60 kbar: a) lattice constant a ; b) lattice constant c ; c) unit cell volume $V = a^2c$; d) the intra-planar As-Fe-As bond angle α as defined in the *inset* (See appendix B for the inter-planar bond angle). Experimental errors on lattice parameters are smaller than symbol dimensions. The black dotted line in panel a, b, and c is a fit to the standard Murnaghan equation of state extended smoothly to negative pressures.¹⁹ From the fits, we extract the moduli of elasticity and report them in appendix C. The black dotted line in panel d is a third order power law fit. In each panel, the horizontal red line marks the lattice parameter of CsFe_2As_2 , and the vertical red line gives the negative pressure required for the lattice parameter of KFe_2As_2 to reach the value in CsFe_2As_2 .

$1.3 \mu\Omega \text{ cm}$, measured here; 3) a CsFe_2As_2 sample (sample 2), with $\rho_0 = 1.5 \mu\Omega \text{ cm}$. Different disorder levels in our samples are due to growth conditions, not to deliberate chemical substitution or impurity inclusions. First, we observe that a 6-fold increase of ρ_0 has negligible impact on P_c in KFe_2As_2 . Secondly, we observe that P_c is 4 kbar smaller in CsFe_2As_2 than in KFe_2As_2 , for samples of comparable ρ_0 . These observations rule out the idea that disorder could be responsible for the lower value of P_c in CsFe_2As_2 compared to KFe_2As_2 .

IV. DISCUSSION

We have established a common trait in CsFe_2As_2 and KFe_2As_2 : both systems have a sudden reversal in the pressure dependence of T_c , with no change in the underlying Fermi surface. The question is: what controls that transition? Why does the low-pressure superconducting state become unstable against the high-pressure state?

In a recent theoretical work by Fernandes and Millis,

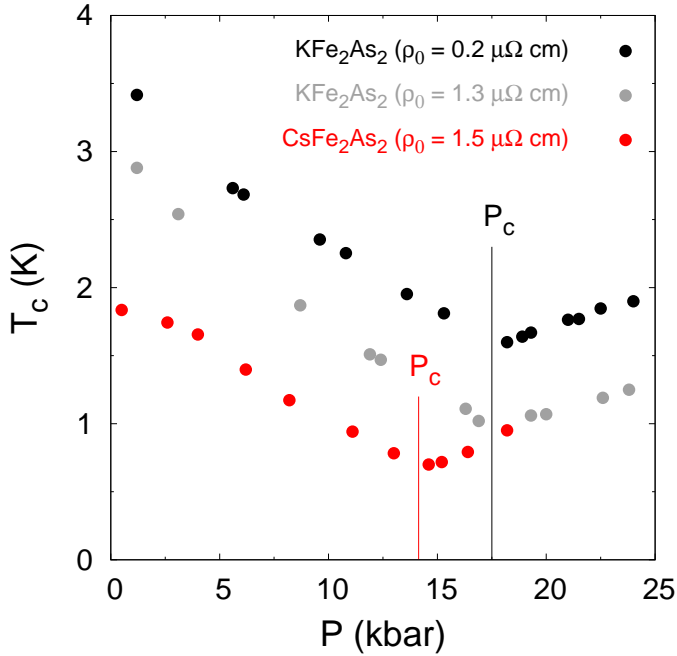


FIG. 4. Pressure dependence of T_c in three samples: pure KFe_2As_2 (black circles), less pure KFe_2As_2 (grey circles), and CsFe_2As_2 (sample 2, red circles). Even though the T_c values for the two KFe_2As_2 samples are different due to different disorder levels, measured by their different residual resistivity ρ_0 , the critical pressure is the same ($P_c = 17.5$ kbar). This shows that the effect of disorder on P_c in KFe_2As_2 is negligible. For comparable ρ_0 , the critical pressure in CsFe_2As_2 , $P_c = 14$ kbar, is clearly smaller than in KFe_2As_2 .

it is demonstrated that different pairing interactions in 122 systems can favour different pairing symmetries.¹¹ In their model, SDW-type magnetic fluctuations, with wavevector $(\pi, 0)$, favour s_{\pm} pairing, whereas Néel-type fluctuations, with wavevector (π, π) , strongly suppress the s_{\pm} state and favour d -wave pairing. A gradual increase in the (π, π) fluctuations eventually causes a phase transition from an s_{\pm} superconducting state to a d -wave state, producing a V-shaped T_c vs P curve.¹¹

In KFe_2As_2 and CsFe_2As_2 , it is conceivable that two such competing interactions are at play, with pressure tilting the balance in favor of one versus the other. We explore such a scenario by looking at how the inelastic scattering evolves with pressure, measured via the inelastic resistivity, defined as $\rho(T) - \rho_0$, where ρ_0 is the residual resistivity. Fig. 5(a) shows raw resistivity data from the KFe_2As_2 sample with $\rho_0 = 1.3 \mu\Omega \text{ cm}$ below 30 K. To extract $\rho(T) - \rho_0$ at each pressure, we make a cut through each curve at $T = 20$ K and subtract from it the residual resistivity ρ_0 that comes from a power-law fit $\rho = \rho_0 + AT^n$ to each curve. ρ_0 is determined by disorder level and does not change as a function of pressure. The resulting $\rho(T = 20 \text{ K}) - \rho_0$ values for this sample are then plotted as a function of normalized pressure P/P_c in Fig. 5(b). Through a similar process we extract the pres-

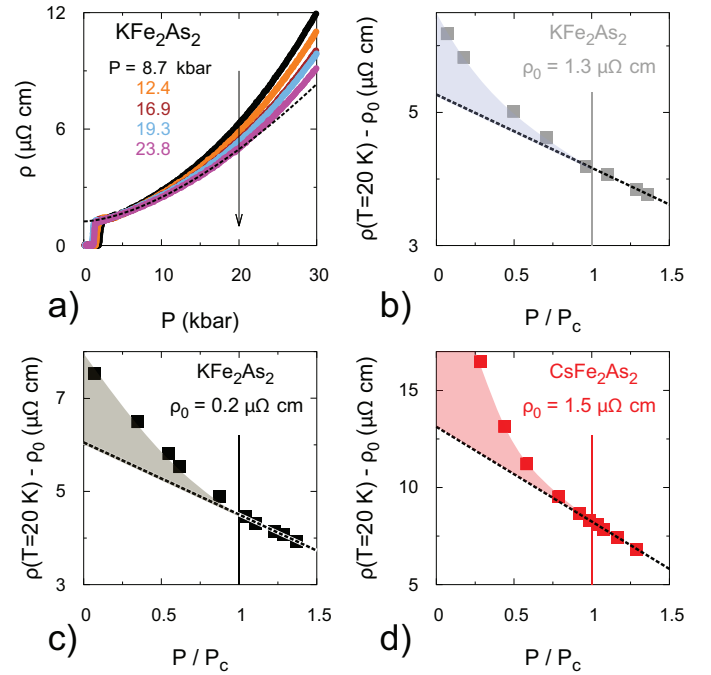


FIG. 5. a) Resistivity data for the KFe_2As_2 sample with $\rho_0 = 1.3 \mu\Omega \text{ cm}$ at five selected pressures. The black vertical arrow shows a cut through each curve at $T = 20$ K and the dashed line is a power law fit to the curve at $P = 23.8$ kbar from 5 to 15 K that is used to extract the residual resistivity ρ_0 . Inelastic resistivity, defined as $\rho(T = 20 \text{ K}) - \rho_0$ is plotted vs P/P_c in b) the less pure KFe_2As_2 sample, c) the purer KFe_2As_2 sample, and d) CsFe_2As_2 (sample 2) where $P_c = 17.5$ kbar for KFe_2As_2 and $P_c = 14$ kbar for CsFe_2As_2 . In panel (b), (c), and (d) the dashed black line is a linear fit to the data above $P/P_c = 1$.

sure dependence of $\rho(20 \text{ K}) - \rho_0$ in CsFe_2As_2 and the purer KFe_2As_2 sample with $\rho_0 = 0.2 \mu\Omega \text{ cm}$ in Fig. 5(c) and (d). In all three samples, at $P/P_c > 1$, the inelastic resistivity varies linearly with pressure. As P drops below P_c , the inelastic resistivity in $(\text{K,Cs})\text{Fe}_2\text{As}_2$ shows a clear rise below their respective P_c , over and above the linear regime. Fig. 5 therefore suggests a connection between the transition in the pressure dependence of T_c and the appearance of an additional inelastic scattering process. Note that our choice of $T = 20$ K for the inelastic resistivity is arbitrary. Resistivity cuts at any finite temperature above T_c give qualitatively similar results.

The Fermi surface of KFe_2As_2 includes three Γ -centered hole-like cylinders. A possible pairing state is an s_{\pm} state where the change of sign occurs between the inner cylinder and the middle cylinder, favored by a small- Q interaction.¹⁰ By contrast, the intraband inelastic scattering wavevectors that favour d -wave pairing are large- Q processes.²⁰ Therefore, one scenario in which to understand the evolution in the inelastic resistivity with pressure (Fig. 5), and its link to the T_c reversal, is the following. At low pressure, the large- Q scattering processes that favor d -wave pairing make a substantial contribu-

tion to the resistivity, as they produce a large change in momentum. These weaken with pressure, causing a decrease in both T_c and the resistivity. This decrease persists until the low- Q processes that favor s_{\pm} pairing, less visible in the resistivity, come to dominate, above P_c .

In summary, we discovered a pressure-induced reversal in the dependence of the transition temperature T_c on pressure in the iron-based superconductor CsFe_2As_2 , similar to our previous finding in KFe_2As_2 . We interpret the T_c reversal at the critical pressure P_c as a transition from one pairing state to another. The fact that P_c in CsFe_2As_2 is smaller than in KFe_2As_2 , even though all lattice parameters would suggest otherwise, shows that structural parameters alone do not control P_c . We also demonstrate that disorder has negligible effect on P_c . Our study of the pressure dependence of resistivity in CsFe_2As_2 and KFe_2As_2 reveals a possible link between T_c and inelastic scattering. Our proposal is that the high-pressure phase in both materials is an s_{\pm} state that changes sign between Γ -centered pockets. As the pressure is lowered, the large- Q inelastic scattering processes that favor d -wave pairing in pure KFe_2As_2 and CsFe_2As_2 grow until at a critical pressure P_c they cause a transition from one superconducting state to another, with a change of pairing symmetry from s -wave to d -wave. The experimental evidence for this is the fact that below P_c the inelastic resistivity, measured as the difference $\rho(20\text{ K}) - \rho_0$, deviates upwards from its linear pressure dependence at high pressure.

ACKNOWLEDGMENTS

We thank A. V. Chubukov, R. M. Fernandes and A. J. Millis for helpful discussions, and S. Fortier for his assistance with the experiments. The work at Sherbrooke was supported by the Canadian Institute for Advanced Research and a Canada Research Chair and it was funded by NSERC, FRQNT and CFI. Work done in China was supported by the National Natural Science Foundation of China (Grant No. 11190021), the Strategic Priority Research Program (B) of the Chinese Academy of Sciences, and the National Basic Research Program of China. Research at the University of Toronto was supported by the NSERC, CFI, Ontario Ministry of Research and Innovation, and Canada Research Chair program. The Canadian Light Source is funded by CFI, NSERC, the National Research Council Canada, the Canadian Institutes of Health Research, the Government of Saskatchewan, Western Economic Diversification Canada, and the University of Saskatchewan.

Appendix A: X-ray data

All our X-ray measurements are performed at room temperature using angle-dispersive technique with the HXMA beam line at CLS. Figure 6 includes two repre-

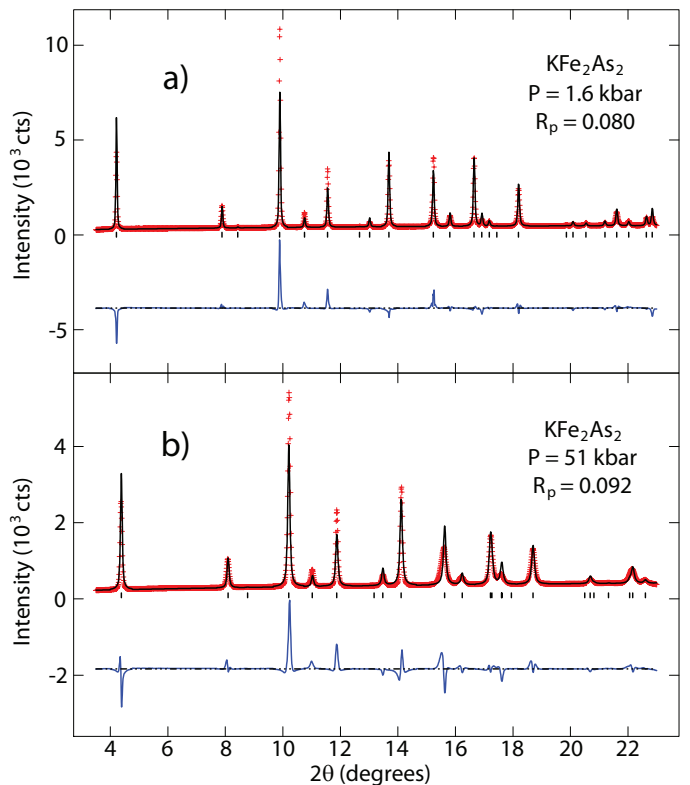


FIG. 6. Representative refinement of the X-ray diffraction patterns collected at a) $P = 1.6$ kbar and b) $P = 51$ kbar. Red crosses show the XRD data plotted as intensity versus 2θ . Black lines are the best fit to the data. Blue lines show the difference between the data and the fits. The goodness of the fit parameter (R_p) is provided for each refinement.

sentative structural refinements of the X-ray diffraction data at $P = 1.6$ kbar and $P = 51$ kbar. 2D diffraction data from the image plate detector were reduced to 1D using the FIT2D program²¹ and plotted as intensity vs 2θ . The structural refinements were performed using the GSAS software package.¹⁷ The experimental data points are illustrated by red crosses, the best fit to the diffraction pattern is illustrated by the solid black line, and the difference between the two curves is denoted by the solid blue line. The Bragg reflections corresponding to the tetragonal $I4/mmm$ structure of KFe_2As_2 are indicated by the black tick marks below the data.

Appendix B: Bond angles

Within the tetragonal structure of KFe_2As_2 , there are two bond angles in each FeAs_4 tetrahedron²² as indicated in the *inset* of Fig. 7: The *intra-planar* bond angle (α) that spans over the bond from one As plane to an Fe atom and back to an As atom in the original plane and the *inter-planar* bond angle (β) that spans over the bond from one As plane through an Fe atom to the next As plane. In the case of an ideal undistorted tetrahe-

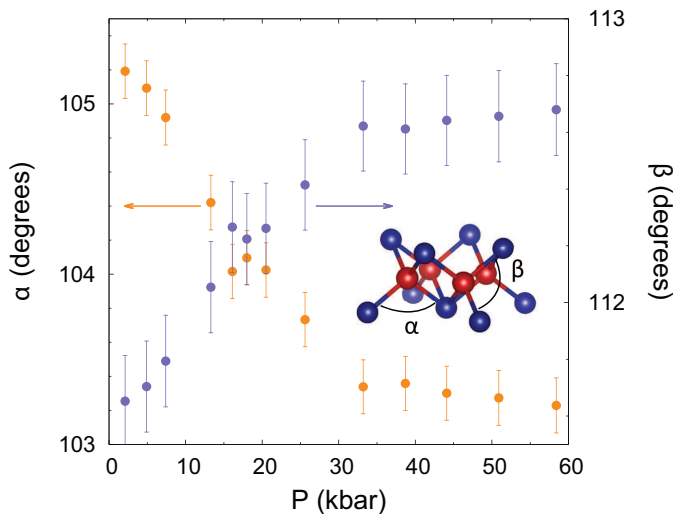


FIG. 7. Pressure dependence of both intra-planar (α) and inter-planar (β) bond angles from 0 to 60 kbar. The values for the two bond angles – defined in the *inset* – are extracted from structural refinements performed on the X-ray data. α decreases as a function of pressure while β increases.

dron $\alpha = \beta = 109.47^\circ$. In Fig. 3(d) we present only the intra-planar bond angle α to show that about -30 kbar is required to tune α from its value in KFe_2As_2 to CsFe_2As_2 . For completeness, here we plot the pressure evolution of both bond angles in Fig. 7. α decreases as a function of pressure while β increases, hence, the size of the tetragonal distortion in KFe_2As_2 grows progressively larger as the pressure increases. Interestingly, the form of this tetragonal distortion is opposite to that observed in $\text{Ca}_{0.67}\text{Sr}_{0.33}\text{Fe}_2\text{As}_2$ where applied pressure causes intra-

layer bond angles to increase and inter-layer bond angles to decrease.²²

Appendix C: Anisotropic compressibility in KFe_2As_2

In Fig. 3, we fit our data to the Murnaghan equation of state:¹⁹

$$P(V) = \frac{K}{K'} \left[\left(\frac{V}{V_0} \right)^{-K'} - 1 \right] \quad (\text{C1})$$

and extend it smoothly to negative pressures to find how much pressure is required to tune the lattice parameters

TABLE I. The moduli of elasticity along a -axis K_a and c -axis K_c as well as the bulk modulus K are extracted by fitting our data to the Murnaghan equation of state. The pressure derivatives of K_a , K_c , and K_V are also reported.

K_a (GPa)	K_c (GPa)	K (GPa)	K'_a	K'_c	K'
105 ± 5	115 ± 3	40 ± 1	400 ± 2	3.3 ± 0.8	6.1 ± 0.4

of KFe_2As_2 to those of CsFe_2As_2 . Note that the compressibility of KFe_2As_2 appears to be anisotropic. The fits also allow us to extract the bulk modulus K and its pressure derivative $K' = \partial K / \partial P$ in KFe_2As_2 . Table I summarizes the values of the bulk modulus K as well as the moduli of elasticity along the a - and c -axes. The modulus of elasticity appears to be almost identical along the a - and the c -axes, but the first derivative of the modulus is over an order of magnitude larger along the a -axis. This accounts for the roughly 40% smaller compression observed for the in-plane lattice constant.

* Fazel.Fallah.Tafti@USherbrooke.ca

† Louis.Taillefer@USherbrooke.ca

¹ J. Zhao, Q. Huang, C. de la Cruz, S. Li, J. W. Lynn, Y. Chen, M. A. Green, G. F. Chen, G. Li, Z. Li, J. L. Luo, N. L. Wang, and P. Dai, *Nature Materials* **7**, 953 (2008).

² M. Rotter, M. Pangerl, M. Tegel, and D. Johrendt, *Angewandte Chemie International Edition* **47**, 79497952 (2008).

³ S. A. J. Kimber, A. Kreyssig, Y.-Z. Zhang, H. O. Jeschke, R. Valent, F. Yokaichiya, E. Colombier, J. Yan, T. C. Hansen, T. Chatterji, R. J. McQueeney, P. C. Canfield, A. I. Goldman, and D. N. Argyriou, *Nature Materials* **8**, 471 (2009).

⁴ P. L. Alireza, Y. T. C. Ko, J. Gillett, C. M. Petrone, J. M. Cole, G. G. Lonzarich, and S. E. Sebastian, *Journal of Physics: Condensed Matter* **21**, 012208 (2009).

⁵ K. Sasmal, B. Lv, B. Lorenz, A. M. Guloy, F. Chen, Y.-Y. Xue, and C.-W. Chu, *Physical Review Letters* **101**, 107007 (2008).

⁶ A. F. Wang, B. Y. Pan, X. G. Luo, F. Chen, Y. J. Yan, J. J. Ying, G. J. Ye, P. Cheng, X. C. Hong, S. Y. Li, and X. H. Chen, *Physical Review B* **87**, 214509 (2013).

⁷ X. C. Hong, X. L. Li, B. Y. Pan, L. P. He, A. F. Wang, X. G. Luo, X. H. Chen, and S. Y. Li, *Physical Review B* **87**, 144502 (2013).

⁸ S. Graser, T. A. Maier, P. J. Hirschfeld, and D. J. Scalapino, *New Journal of Physics* **11**, 025016 (2009).

⁹ S. Maiti, M. M. Korshunov, T. A. Maier, P. J. Hirschfeld, and A. V. Chubukov, *Physical Review Letters* **107**, 147002 (2011).

¹⁰ S. Maiti, M. M. Korshunov, and A. V. Chubukov, *Physical Review B* **85**, 014511 (2012).

¹¹ R. M. Fernandes and A. J. Millis, *Physical Review Letters* **110**, 117004 (2013).

¹² F. F. Tafti, A. Juneau-Fecteau, M.-. Delage, S. Ren de Cotret, J.-P. Reid, A. F. Wang, X.-G. Luo, X. H. Chen, N. Doiron-Leyraud, and L. Taillefer, *Nature Physics* **9**, 349 (2013).

¹³ T. Terashima, K. Kihou, K. Sugii, N. Kikugawa, T. Matsumoto, S. Ishida, C.-H. Lee, A. Iyo, H. Eisaki, and S. Uji, *arXiv:1401.6257 [cond-mat]* (2014).

¹⁴ J.-P. Reid, M. A. Tanatar, A. Juneau-Fecteau, R. T. Gordon, S. R. de Cotret, N. Doiron-Leyraud, T. Saito,

- H. Fukazawa, Y. Kohori, K. Kihou, C. H. Lee, A. Iyo, H. Eisaki, R. Prozorov, and L. Taillefer, *Physical Review Letters* **109**, 087001 (2012).
- ¹⁵ J. K. Dong, S. Y. Zhou, T. Y. Guan, H. Zhang, Y. F. Dai, X. Qiu, X. F. Wang, Y. He, X. H. Chen, and S. Y. Li, *Physical Review Letters* **104**, 087005 (2010).
- ¹⁶ K. Hashimoto, A. Serafin, S. Tonegawa, R. Katsumata, R. Okazaki, T. Saito, H. Fukazawa, Y. Kohori, K. Kihou, C. H. Lee, A. Iyo, H. Eisaki, H. Ikeda, Y. Matsuda, A. Carrington, and T. Shibauchi, *Physical Review B* **82**, 014526 (2010).
- ¹⁷ A. Larson and R. Von Dreele, Los Alamos National Laboratory Report LAUR 86-748 (2000).
- ¹⁸ S. L. Bud'ko, M. Sturza, D. Y. Chung, M. G. Kanatzidis, and P. C. Canfield, *Physical Review B* **87**, 100509 (2013).
- ¹⁹ F. D. Murnaghan, *American Journal of Mathematics* **59**, 235 (1937).
- ²⁰ R. Thomale, C. Platt, W. Hanke, J. Hu, and B. A. Bernevig, *Physical Review Letters* **107**, 117001 (2011).
- ²¹ A. P. Hammersley, S. O. Svensson, M. Hanfland, A. N. Fitch, and D. Hausermann, *High Pressure Research* **14**, 235 (1996).
- ²² J. R. Jeffries, N. P. Butch, K. Kirshenbaum, S. R. Saha, G. Samudrala, S. T. Weir, Y. K. Vohra, and J. Paglione, *Physical Review B* **85**, 184501 (2012).